*Solid State Science and Technology, Vol. 34, No. 2 (2026) 186-198*
*https://doi.org/10.66514/ssst34-2-186-198*

# Effect of Heat Treatment and SrO Co-doping on the Thermoluminescence of $Dy_2O_3$-Doped $MgSO_4$ Powder Irradiated with $^{241}Am$ Gamma Rays

*Izleen Laili Ibrahim[1], Iskandar Shahrim Mustafa[1,*], Muhammad Fadhirul Izwan Abdul Malik[2], Hayder Salah Naeem[3], G. I. Efenji[4]*

*[1]School of Physics, Universiti Sains Malaysia, 11800 USM, Penang, Malaysia*
*[2]Science and Engineering Research Center, USM Engineering Campus, Universiti Sains Malaysia, 14300 Nibong Tebal, Malaysia*
*[3]Science Department, College of Basic Education, Al-Muthanna University, 66001 Samawah, Al Muthanna, Iraq*
*[4]Federal University Lokoja, P.M.B. 1154, Lokoja, Kogi State, Nigeria*

**Corresponding author (email: iskandarshah@usm.my)*

*(Received: 8 October 2026 / Revised:12 November 2026 / Accepted: 17 November 2026 / Published online: 19 November 2026)*

*© The Author(s) 2026. This article is licensed under a Creative Commons Attribution 4.0 International License (CC BY 4.0)*

## ABSTRACT

Magnesium sulphate is an inexpensive host for thermoluminescence (TL) dosimetry, but its intrinsic sensitivity is low. Dy doping is known to sensitize $MgSO_4$, but the effects of SrO co-doping and of the heat-treatment temperature on $Dy_2O_3$-doped $MgSO_4$ powder have not been reported, and its response to low-energy photons at the microgray doses relevant to occupational monitoring has received little attention. In this work, $MgSO_4$ powders containing $Dy_2O_3$ (about 3.9 mol%) and SrO ($x$ = 0, 0.03 and 0.05, corresponding to 0, 2.5 and 4.2 mol% in the batch) were prepared by solid-state mixing and heat treatment at 400, 800 and 900 °C for 6 h. FESEM showed micrometer-sized angular particles after treatment at 400 °C and partially sintered, agglomerated particles at 800–900 °C. EDX confirmed the presence of Mg, S, O, Dy and Sr, but the Dy content varied widely between samples, indicating incomplete homogenization. Aliquots were irradiated with 59.5 keV gamma rays from a 3.5 GBq $^{241}Am$ source for 15–60 min (nominal doses 50–200 μGy) and read with a Harshaw 3500 reader at 10 °C $s^{-1}$ to 300 °C. The powders treated at 400 °C showed no glow peak, and their integrated signal (3–6 nC) was at the reader background level. Treatment at 800 and 900 °C produced a strong glow peak that was still rising when the readout reached 300 °C, together with a weaker shoulder at about 175–250 °C. At 800 °C, SrO co-doping increased the mean integrated TL about three-fold (from 19 to 58–64 nC), and raising the treatment temperature from 800 to 900 °C increased it a further 9–19-fold. Within 50–200 μGy, the integrated TL did not increase systematically with dose ($R^2 \leq 0.68$, aliquot-to-aliquot variation 5–78%); only the 800 °C, $x$ = 0.03 powder showed a positive trend (0.20 nC $\mu Gy^{-1}$, $R^2$ = 0.36). Heat treatment at 800–900 °C and SrO co-doping clearly

sensitize $MgSO_4$:Dy, but a higher readout temperature, mass-normalized replicate aliquots and calibrated irradiations are needed to establish its dose response.

***Keywords:*** Thermoluminescence; magnesium sulphate; dysprosium; strontium oxide; powder dosimeter

## INTRODUCTION

Ionizing radiation is used routinely in diagnostic radiology, nuclear medicine and radiotherapy, and the occupational exposure of the staff involved must be monitored to keep doses below the recommended limit of 20 mSv per year [1]. Thermoluminescence dosimeters (TLDs) are widely used for this purpose because they are small, passive, reusable and sensitive from the microgray to the gray range [2,3]. In a TL material, charge carriers produced by irradiation are captured at defect-related traps and released on heating, and the resulting luminescence is proportional to the absorbed dose over a useful range [4,5]. TL phosphors in powder form are attractive because the amount of material can be adjusted and the powder can be placed in holders of any shape, for example for surface-dose or mailed-dose measurements [6,7].

Sulphate phosphors doped with rare-earth ions, notably $CaSO_4$:Dy, are among the most sensitive TL materials [3]. Magnesium sulphate is inexpensive, readily available and has a lower effective atomic number than $CaSO_4$, but undoped $MgSO_4$ has poor TL sensitivity [8]. Doping with dysprosium greatly improves its response: $MgSO_4$:Dy nanorods and microcrystalline powders prepared by solid-state reaction show well-defined glow peaks and, at the optimum Dy content of about 0.3 mol%, a sensitivity several times higher than that of LiF:Mg,Ti (TLD-100) [9,10]. $Dy^{3+}$ acts as an efficient luminescence center and introduces trapping levels in the band gap of oxide and sulphate hosts [11–13].

Strontium is an effective co-dopant for several TL hosts. In $Al_2O_3$ and in Cu-doped lithium magnesium borate glass, the glow-peak intensity increases with Sr concentration up to an optimum and then decreases [14,15], and Sr-containing barium sulphate co-doped with Dy and Tb shows a linear gamma-ray response over a wide dose range [16]. Recent work on sulphate TL phosphors has concentrated on co-doped $CaSO_4$, for example $CaSO_4$:Dy,Eu [17], $CaSO_4$:Tb,Eu [18] and $CaSO_4$:Mn,Tb [19,20], on Eu-doped $MgSO_4$ [21], and on $MgSO_4$:$Dy_2O_3$ incorporated in borate glass ceramics [22,23]. The larger $Sr^{2+}$ ion (1.18 Å compared with 0.72 Å for $Mg^{2+}$ in six-fold coordination) [24] is expected to distort the $MgSO_4$ lattice and create additional trapping sites, but the effect of SrO co-doping on $MgSO_4$:Dy has not been reported.

The heat-treatment temperature also controls the incorporation of dopants, the defect structure, the crystallinity and the grain size of solid-state phosphors, and hence their TL sensitivity [25]. This study therefore examines the morphology, composition and TL response of $Dy_2O_3$-doped $MgSO_4$ powders co-doped with SrO and heat-treated at 400, 800 and 900 °C, using low-dose irradiation with 59.5 keV gamma rays from $^{241}Am$.

## MATERIALS AND METHODS

*Sample preparation*

Magnesium sulfate heptahydrate (*ReagentPlus*®, ≥99.0%; Sigma-Aldrich, cat. no. 10034-99-8), strontium oxide (SrO) with 99.9% trace metals basis (Sigma-Aldrich, cat. no. 1314-11-0) and dysprosium (III) oxide ($Dy_2O_3$) powders 99.9% trace metals basis (Sigma-Aldrich, cat. no. 1308-87-8) were used as received. Three compositions, designated by the nominal SrO fraction $x$ in $[(MgSO_4)_{0.95}(Dy_2O_3)_{0.05}]_{1-x}(SrO)_x$ with $x = 0$, 0.03 and 0.05, were prepared as 6 g batches by solid-state mixing followed by heat treatment, following the general solid-state route used for sulphate TL phosphors [10,20,21] (Table 1). The batch weights correspond to 0, 2.5 and 4.2 mol% SrO and about 3.9 mol% $Dy_2O_3$ (11 wt.%). The powders were weighed, transferred to Coors™ high-alumina crucible with the volume capacity of 50 mL and mixed thoroughly with a glass rod; the spatula and rod were cleaned with ethanol between samples to avoid cross-contamination.

Table 1. Batch weights (g) and the corresponding SrO and $Dy_2O_3$ contents (mol%) of the 6 g batches

| $x$ | $MgSO_4$ (g) | SrO (g) | $Dy_2O_3$ (g) | SrO (mol%) | $Dy_2O_3$ (mol%) |
|---|---|---|---|---|---|
| 0 | 5.32 | 0.00 | 0.68 | 0 | 3.96 |
| 0.03 | 5.21 | 0.12 | 0.67 | 2.50 | 3.88 |
| 0.05 | 5.14 | 0.20 | 0.66 | 4.16 | 3.81 |

The mol% values were calculated from the batch weights by assuming anhydrous $MgSO_4$ (120.37 g $mol^{-1}$)

Each composition was heat-treated in an electric furnace (Nabertherm, P330 controller) at 400, 800 or 900 °C, giving nine samples. The furnace was heated to 400 °C in 37 min and from 400 to 800 °C in a further 45 min, held at the target temperature for 6 h and then allowed to cool naturally to room temperature overnight. The powders were stored in labelled zip-lock bags until use.

*Morphology and composition*

The morphology and elemental composition of the powders were examined with a field-emission scanning electron microscope (FEI Nova NanoSEM 450) equipped with an energy-dispersive X-ray (EDX) spectrometer at the Nano-Optoelectronics Research and Technology Laboratory (NOR Lab), School of Physics, Universiti Sains Malaysia [26], as in our earlier work on Mg-based TL materials [22,27]. Small amounts of powder were mounted on carbon tape and imaged at accelerating voltages of 5–10 kV. A magnification of 40,000× was used to resolve the sub-micrometer surface features (fine grains of 0.1–0.3 μm and necks between particles) on which the comparison of heat-treatment temperatures is based. Lower-magnification images were not recorded, so the particle- and agglomerate-size distributions were not quantified.

*Irradiation and TL readout*

Each sample was divided into four aliquots, which were irradiated with a sealed $^{241}Am$ source (model AMC 8726; 100 mCi on 7 August 1990, about 3.5 GBq at the time of the

experiment) emitting 59.54 keV gamma rays [28]. The aliquots were irradiated for 15, 30, 45 and 60 min, corresponding to nominal doses of 50, 100, 150 and 200 μGy. A nominal absorbed dose rate of about 200 μGy $h^{-1}$ was achieved at the irradiation position with a Cs-137 gamma source. Each of the nine samples was prepared as a single batch. For each sample, one aliquot (approximately 20 mg) was irradiated at each nominal dose and read once, giving four readings per sample; replicate aliquots at the same dose were not measured. FESEM images and EDX spectra were acquired from one field and one area of each sample, respectively.

The TL signal was read with a Harshaw TLD 3500 reader. Powder (approximately 20 mg, dispensed by spatula) was transferred with a spatula into 120 μL aluminum pan and onto the TLD planchet. The planchet, and tools were cleaned with alcohol swabs between readings. The time–temperature profile, chosen following standard TL readout practice [3,4] and earlier work on $MgSO_4$:Dy [10], used a preheat at 50 °C, a linear heating rate of 10 °C $s^{-1}$ to a maximum temperature of 300 °C, and a total acquisition time of 100 s (25 s of heating followed by 75 s at 300 °C), recorded in 200 channels of 0.5 s. A post-readout anneal at 300 °C for 120 s was applied. The integrated charge over the full acquisition was taken as the TL response, and the dose response was evaluated by linear regression of the integrated charge against nominal dose. The coefficient of variation (CV) was calculated as the standard deviation of the four aliquots of a sample divided by their mean.

## RESULTS AND DISCUSSION

*Elemental composition*

EDX detected only O, Mg, S, Sr and Dy (Table 2). For the 400 °C, $x = 0$ sample, the measured composition (66.1 at% O, 16.0 at% Mg, 16.1 at% S, 1.9 at% Dy) agrees closely with the nominal values, and the S/Mg atomic ratio remained between 0.8 and 1.4 for all samples, consistent with retention of the sulphate after treatment at up to 900 °C.

Table 2. Elemental composition (at%) of the powders determined by EDX, compared with the nominal composition calculated from the batch weights

| *T* (°C) | *x* | O | Mg | S | Sr | Dy |
|---|---|---|---|---|---|---|
| Nominal | 0 | 66.45 | 16.11 | 16.11 | 0 | 1.33 |
| Nominal | 0.03 | 66.30 | 15.97 | 15.97 | 0.43 | 1.33 |
| Nominal | 0.05 | 66.21 | 15.88 | 15.88 | 0.72 | 1.32 |
| 400 | 0 | 66.08 | 15.97 | 16.09 | 0 | 1.87 |
| 400 | 0.03 | 55.19 | 12.38 | 14.60 | 0.46 | 17.37 |
| 400 | 0.05 | 63.41 | 10.12 | 13.42 | 0.12 | 12.93 |
| 800 | 0 | 60.07 | 14.26 | 19.93 | 0.10 | 5.64 |
| 800 | 0.03 | 60.50 | 19.26 | 15.02 | 1.13 | 4.09 |
| 800 | 0.05 | 64.10 | 16.71 | 18.34 | 0.02 | 0.82 |
| 900 | 0 | 60.38 | 13.00 | 18.41 | 0 | 8.21 |
| 900 | 0.03 | 61.27 | 19.53 | 18.04 | 0.02 | 1.14 |
| 900 | 0.05 | 61.98 | 13.15 | 13.71 | 0.93 | 10.23 |

EDX analysis is semi-quantitative; values are from a single area of each sample

The Dy content, however, ranged from 0.8 to 17.4 at% against a nominal 1.3 at%, and the Sr content of the co-doped samples (0.02–1.13 at%) also scattered about its nominal value (0.43–0.72 at%). The Sr signal of 0.10 at% in the 800 °C, $x$ = 0 sample is at the detection limit of EDX and is not significant. Because EDX samples only a few cubic micrometers, this scatter indicates that the $Dy_2O_3$ and SrO particles were not homogeneously distributed in the $MgSO_4$, as expected for mixing with a glass rod without grinding.

*Morphology*

After treatment at 400 °C, the powders consisted of angular, plate-like particles a few micrometers across with sharp edges and layered surfaces (Figure 1(a)–(c)). Treatment at 800 °C produced more compact particles with stepped surfaces (Figure 1(d)) and, for $x$ = 0.03, a large population of fine, rounded grains of about 0.1–0.3 µm on the particle surfaces (Figure 1(e)). At 900 °C, the particles were partially sintered into agglomerates with smoother, fused surfaces (Figure 1(g)–(i)). The progressive rounding and necking of the particles indicate surface diffusion and the onset of sintering above 800 °C, which would also promote the incorporation of Dy and Sr into the host lattice.

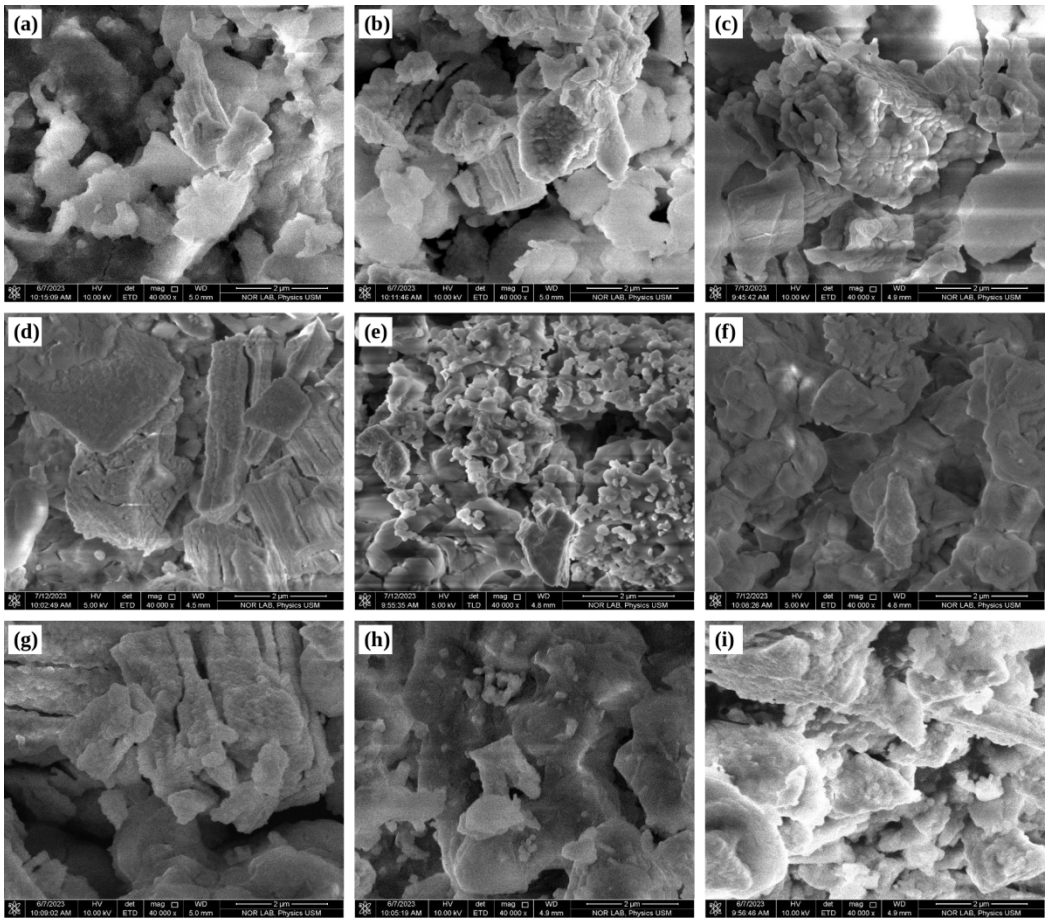



Figure 1. FESEM images (40,000×, scale bar 2 µm) of powders heat-treated at 400 °C (a–c), 800 °C (d–f) and 900 °C (g–i), with $x$ = 0 (left), 0.03 (center) and 0.05 (right)

These observations differ from the morphology of $MgSO_4$:Dy prepared by wet chemistry: the semi-co-precipitation route produced nanorods [9], whereas the micrometer-sized angular particles obtained here are inherited from the commercial starting powders and modified only by heat treatment. A strong dependence of grain morphology on the preparation route has likewise been reported for $CaSO_4$:Mn,Tb prepared by four routes, including solid-state diffusion [20]. The progressive rounding, necking and agglomeration with increasing temperature agree with reports for other phosphors, in which grain size increased with annealing temperature together with crystallinity and TL intensity [25], and with the particle-growth-assisted TL enhancement reported for $Dy_2O_3$-doped phosphate glasses [11]. The fine 0.1–0.3 μm grains seen only on the 800 °C, $x = 0.03$ particles (Figure 1(e)) may be undissolved SrO or $Dy_2O_3$, which would be consistent with the inhomogeneous dopant distribution found by EDX (Section 3.1); EDX mapping would be needed to confirm this.

*Glow curves*

Figure 2 shows the glow curves recorded by the reader. The powders treated at 400 °C (Figure 2(a)–(c)) showed no glow peak: the signal remained at 0.03–0.1 nA throughout the readout, comparable to the photomultiplier dark current and thermal background, with occasional single-channel spikes. Their integrated charge (3–6 nC; Table 3) therefore represents the reader background rather than radiation-induced TL.

After treatment at 800 and 900 °C, all powders showed a weak shoulder between channels 25 and 40 (about 175–250 °C) followed by an intense peak at channels 55–75, i.e. 2.5–12.5 s after the heating ramp had reached 300 °C (Figures 2(d)–2(i)). The main peak therefore corresponds to traps that are only emptied at or above 300 °C, and the main glow peak lies above the maximum readout temperature: it appears during the isothermal hold rather than during the linear ramp. This is consistent with earlier studies of $MgSO_4$:Dy, whose glow curves contain components at about 140, 190, 260 and 360 °C; for $MgSO_4$:Dy,P, the main dosimetric peak lies at about 284 °C, with a satellite at about 353 °C, when read at 5 °C $s^{-1}$ [8].

The weak shoulder at 175–250 °C observed here corresponds to the lower-temperature components, and the main peak, which appears only after the readout reaches 300 °C, to the ≈350–360 °C component. The higher heating rate used here (10 °C $s^{-1}$, compared with 2 °C $s^{-1}$ in [10] and 5 °C $s^{-1}$ in [8]) shifts glow peaks to higher temperatures and increases the thermal lag between planchet and powder [3], which further favors the appearance of this peak during the isothermal hold. The peak intensity increased with SrO co-doping at 800 °C (0.5 nA for $x = 0$, compared with 2.5 and 2.2 nA for $x = 0.03$ and 0.05) and increased by roughly an order of magnitude at 900 °C (24, 38 and 45 nA for $x = 0$, 0.03 and 0.05). High-temperature glow peaks are desirable for dosimetry because the corresponding traps are thermally stable and fade slowly at room temperature [3,4]. However, recording the complete peak will require a readout to at least 400 °C, and plotting the signal against temperature, as is usual, is not meaningful when the peak occurs during the isothermal hold.

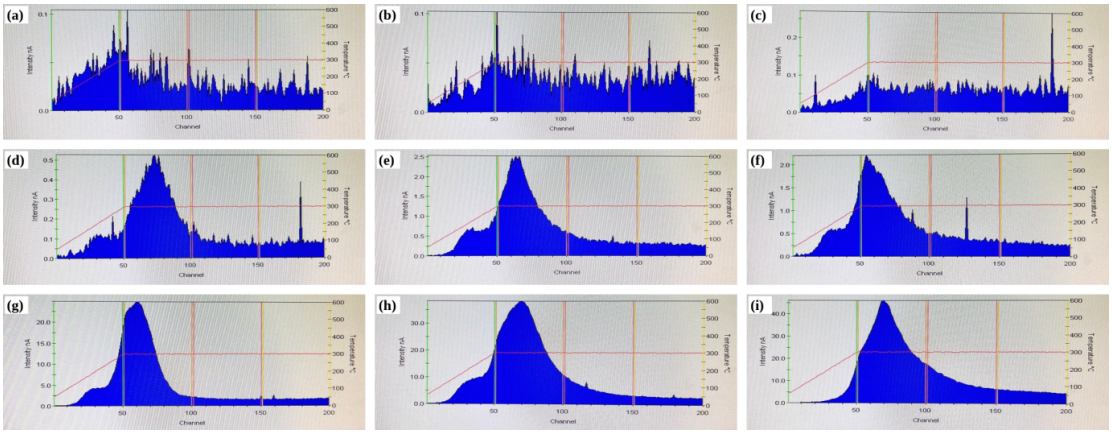


Figure 2. Glow curves recorded by the reader (intensity in nA versus channel; red line, heating profile, right axis in °C) for powders treated at 400 °C (a–c), 800 °C (d–f) and 900 °C (g–i), with $x$ = 0 (left), 0.03 (center) and 0.05 (right). Each channel is 0.5 s; the temperature reaches 300 °C at channel 50

*Integrated TL response*

The integrated charges (Table 3 and Figure 3) confirm the strong effect of heat treatment. Averaged over the four aliquots, the response rose from 3–6 nC at 400 °C to 19–64 nC at 800 °C and 366–851 nC at 900 °C, i.e. 9–19 times higher at 900 °C than at 800 °C for the same composition. Two effects are likely to contribute. At 400 °C, the dopant oxides cannot diffuse appreciably into the $MgSO_4$, so few $Dy^{3+}$ luminescence centers and associated traps are formed; at 800–900 °C, solid-state diffusion and sintering (Figure 1) allow $Dy^{3+}$ and $Sr^{2+}$ to substitute for $Mg^{2+}$, creating charge-compensating defects that act as traps [8,10]. Growth and fusion of the particles may also reduce non-radiative recombination at surfaces, as reported for Dy-doped phosphate glasses [11]. A similar increase of TL intensity with annealing temperature, accompanied by grain growth, has been reported for $Ca_2Al_2SiO_7:Ce^{3+}$ annealed at 1073–1373 K [25].

SrO co-doping increased the mean response at 800 °C by factors of 3.3 ($x$ = 0.03) and 3.0 ($x$ = 0.05), with no overlap between the ranges of the four aliquots; at 900 °C the mean increased by factors of 1.6 and 2.3, but the ranges overlap, so this increase is less certain. The substitution of the much larger $Sr^{2+}$ ion for $Mg^{2+}$ [24] would distort the lattice and introduce additional trapping sites. The slightly lower response of $x$ = 0.05 than $x$ = 0.03 at 800 °C is consistent with the rise-then-fall behavior reported for Sr co-doping in other hosts [14,15], although the aliquot-to-aliquot scatter is too large to locate an optimum reliably. Sensitization by a second dopant with an optimum content has also been reported recently for sulphate phosphors: in $CaSO_4$:Dy,Eu the highest sensitivity was obtained at the lowest Eu content studied ($x$ = 0.05) [17] and in $CaSO_4$:Tb,Eu the dopant contents controlled the luminescence intensity [18]. The $Dy_2O_3$ content used here (about 3.9 mol%) is more than ten times the optimum of 0.3 mol% reported for $MgSO_4$:Dy [10], so the sensitivity may be further limited by concentration quenching.

Table 3. Integrated TL charge (nC) for nominal doses of 50–200 µGy, with the mean, coefficient of variation (CV) across the four aliquots, and the slope and $R^2$ of a linear fit against dose

| $T$ | $x$ | 50 µGy | 100 | 150 | 200 | Mean | CV | Slope (nC | $R^2$ |
|---|---|---|---|---|---|---|---|---|---|
| 400 | 0 | 3.14 | 2.95 | 2.87 | 3.15 | 3.03 | 5 | −0.0001 | 0.00 |
| 400 | 0.03 | 3.43 | 3.75 | 3.25 | 3.19 | 3.40 | 7 | −0.0024 | 0.39 |
| 400 | 0.05 | 5.74 | 4.76 | 6.15 | 6.23 | 5.72 | 12 | 0.0057 | 0.30 |
| 800 | 0 | 14.37 | 26.22 | 14.47 | 21.56 | 19.2 | 30 | 0.0196 | 0.05 |
| 800 | 0.03 | 64.74 | 34.10 | 71.52 | 85.90 | 64.1 | 34 | 0.2018 | 0.36 |
| 800 | 0.05 | 60.74 | 53.49 | 63.22 | 53.90 | 57.8 | 8 | −0.0216 | 0.08 |
| 900 | 0 | 497.00 | 187.50 | 703.30 | 77.00 | 366 | 78 | −1.4884 | 0.11 |
| 900 | 0.03 | 1043.00 | 387.20 | 374.10 | 529.40 | 583 | 54 | −3.1078 | 0.41 |
| 900 | 0.05 | 1219.00 | 1350.00 | 362.40 | 470.80 | 851 | 59 | −6.4644 | 0.68 |

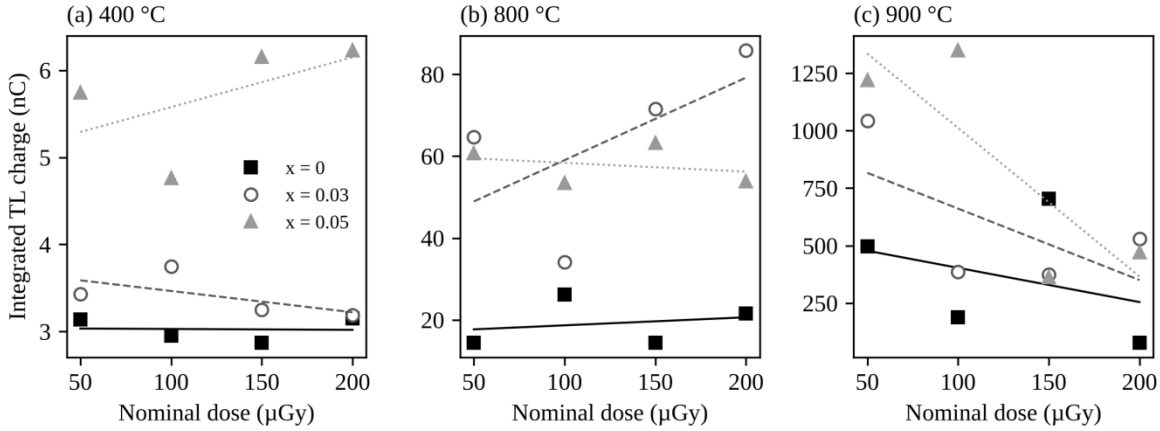



Figure 3. Integrated TL charge versus nominal dose for powders heat-treated at (a) 400 °C, (b) 800 °C and (c) 900 °C. Lines are least-squares linear fits

In contrast to the clear effects of heat treatment and co-doping, the integrated charge did not increase systematically with nominal dose for any sample. The coefficient of variation between the four aliquots of each sample (5–78%) was comparable to or larger than the four-fold change in nominal dose, the linear fits had $R^2 \leq 0.68$, and six of the nine slopes were negative. The 800 °C, $x = 0.03$ powder showed the largest positive slope (0.20 nC µGy$^{-1}$, $R^2 = 0.36$), but this is not sufficient to demonstrate a linear dose response. Earlier studies established the dose response of $MgSO_4$-based phosphors at much higher doses: 0.1 Gy–20 kGy (supralinear) for $MgSO_4$:Dy,P [8], linear up to 10 kGy for $MgSO_4$:Dy nanorods [9] and linear over 0.1–50 Gy for $MgSO_4$:Eu [21]. The nominal doses used here (50–200 µGy) are more than two orders of magnitude below the lowest of these, so the dose-dependent part of the signal is expected to be small compared with the aliquot-to-aliquot variation. Several experimental factors can account for this scatter. First, the main glow peak lies above the 300 °C maximum readout temperature, so the integrated charge depends on how much of the peak is emptied during the isothermal hold, which is sensitive to the

thermal contact between powder and planchet. Second, the mass of powder in each reading was not controlled, and TL output is proportional to the irradiated mass. Third, the inhomogeneous distribution of Dy and Sr shown by EDX means that aliquots taken from the same batch can differ in sensitivity.

The dependence of reproducibility on the preparation route has been demonstrated for $CaSO_4$:Mn,Tb, for which slow evaporation gave CVs below 10%, whereas the high CVs of sol-gel and co-precipitated phosphors limited their reproducibility [20]; the CVs of 5–78% found here for mixed but unground powders point to homogenization as the first priority. Finally, unirradiated (zero-dose) aliquots were not included in the experimental design, so the background and any signal from residual or environmental dose, handling or light exposure could not be subtracted sample by sample. The 400 °C powders, which show no glow peak, give an approximate measure of the reader background under the same readout conditions (3–6 nC, CV 5–12%; Table 3). This is one to two orders of magnitude below the signals of the 800 and 900 °C powders (19–851 nC) and cannot account for the effects of heat treatment or co-doping, but sample-specific contributions of similar or larger size cannot be excluded, which is a further reason why the dose response could not be resolved. The supralinear and sublinear regions discussed for TL materials at higher doses [5] cannot be identified from these data.

*Limitations of the present study*

This work was designed as a screening study of composition and heat-treatment temperature, and its design limits the conclusions that can be drawn. Each composition–temperature combination was prepared as a single batch; one aliquot was read per dose, with no replicates at the same dose and no unirradiated (zero-dose) aliquots; EDX and FESEM were obtained from a single area and at a single magnification; the readout was limited to 300 °C, below the main glow peak; the doses are nominal values that were not verified with a reference dosimeter; and no XRD phase analysis was performed. The effects of heat treatment (9–19-fold between 800 and 900 °C) and of SrO co-doping at 800 °C (about three-fold) are larger than the spread of the four aliquots of each sample, whose ranges do not overlap (Table 3), and are therefore considered robust. The SrO effect at 900 °C, where the ranges overlap, and the dose response are not established by the present data and require the replicated, mass-normalized and zero-dose-corrected measurements outlined in Section 4.

## CONCLUSIONS

$Dy_2O_3$-doped $MgSO_4$ powders co-doped with 0–4.2 mol% SrO were prepared by solid-state mixing and heat treatment at 400, 800 and 900 °C, and their TL response to 59.5 keV gamma rays from $^{241}$Am was examined. The main findings are as follows:

(i) EDX confirmed the expected elements and retention of the sulphate up to 900 °C, but the Dy and Sr contents varied widely between samples, showing that simple mixing did not distribute the dopants homogeneously.

(ii) Powders treated at 400 °C showed no TL above the reader background. Treatment at 800 and 900 °C produced a strong glow peak above 300 °C, with a weaker shoulder at about 175–250 °C, together with partial sintering of the particles.

(iii) The mean integrated TL increased about three-fold with SrO co-doping at 800 °C and a further 9–19-fold when the treatment temperature was raised to 900 °C.
(iv) Within the nominal dose range of 50–200 μGy, the integrated TL did not vary systematically with dose because of large aliquot-to-aliquot variation.

Heat treatment at 900 °C and SrO co-doping are therefore effective in sensitizing $MgSO_4$:Dy powder. To establish the dosimetric properties, future work should use homogenized (ground) batches with lower $Dy_2O_3$ contents, XRD phase analysis, readout to at least 400 °C, mass-normalized replicate aliquots including zero-dose controls, and irradiations calibrated against a reference dosimeter over a wider dose range, followed by fading and reproducibility tests.

## ACKNOWLEDGEMENTS

The authors thank the School of Physics, Universiti Sains Malaysia for funding this work, Encik Rizal and Puan Aida for laboratory assistance and the Nano-Optoelectronics Research and Technology Laboratory (NOR Lab) for FESEM–EDX analysis.

## AUTHOR CONTRIBUTIONS

Izleen Laili Ibrahim: investigation, data curation, formal analysis, writing – original draft. Iskandar Shahrim Mustafa: conceptualization, methodology, supervision, resources, writing – review and editing. Muhammad Fadhirul Izwan Abdul Malik: data curation, formal analysis. Hayder Salah Naeem: investigation, data curation. G. I. Efenji: data curation, formal analysis. All authors have read and approved the final manuscript.

## CONFLICT OF INTEREST

The authors declare no conflict of interest.

## DATA AVAILABILITY

The data supporting the findings of this study are available from the corresponding author upon reasonable request.

## REFERENCES

[1] International Commission on Radiological Protection. The 2007 recommendations of the International Commission on Radiological Protection. ICRP Publication 103. *Ann ICRP*. 2007;37(2–4):1–332. https://doi.org/10.1016/j.icrp.2007.10.003

[2] Izewska J, Rajan G. Radiation dosimeters. In: Podgorsak EB, (ed.) *Radiation Oncology Physics: A Handbook for Teachers and Students*. Vienna: International Atomic Energy Agency; 2005. p. 71–99. https://www.iaea.org/node/40955

[3] McKeever SWS. *Thermoluminescence of Solids*. Cambridge: Cambridge University Press; 1985. https://doi.org/10.1017/CBO9780511564994

[4] Bos AJJ. Theory of thermoluminescence. *Radiation Measurements.* 2006;41(Suppl. 1):S45–56. https://doi.org/10.1016/j.radmeas.2007.01.003

[5] Lawless JL, Chen R, Pagonis V. Sublinear dose dependence of thermoluminescence and optically stimulated luminescence prior to the approach to saturation level. *Radiation Measurements.* 2009;44(5–6):606–10. https://doi.org/10.1016/j.radmeas.2009.03.003

[6] Rapley P. Surface dose measurement using TLD powder extrapolation. *Medical Dosimetry.* 2006;31(3):209–15. https://doi.org/10.1016/j.meddos.2006.02.003

[7] Rah JE, Hong JY, Kim GY, Kim YL, Shin DO, Suh TS. A comparison of the dosimetric characteristics of a glass rod dosimeter and a thermoluminescent dosimeter for mailed dosimeter. *Radiation Measurements.* 2009;44(1):18–22. https://doi.org/10.1016/j.radmeas.2008.10.010

[8] Luo DL, Yu KN, Zhang CX, Li GZ. Thermoluminescence characteristics and dose responses in $MgSO_4$:Dy,P and $MgSO_4$:Dy,P,Cu phosphors. *Journal of Physics D: Applied Physics.* 1999;32(23):3068–74. https://doi.org/10.1088/0022-3727/32/23/313

[9] Zahedifar M, Almasifard F, Sadeghi E, Kashefi Biroon M, Ramazani-Moghaddam-Arani A. Thermoluminescence kinetic analysis and dosimetry features of $MgSO_4$:Dy and $MgSO_4$:Cu nano-rods. *Radiation Physics and Chemistry.* 2016;125:127–33. https://doi.org/10.1016/j.radphyschem.2016.04.005

[10] Zahedifar M, Almasifard F, Sadeghi E, Harooni S, Kashefi Biroon M. Thermoluminescence dosimetry properties and kinetic analysis of $MgSO_4$:Dy microcrystalline prepared by solid state method. *Radiation Measurements.* 2017;103:26–32. https://doi.org/10.1016/j.radmeas.2017.06.006

[11] Gasiorowski A, Szajerski P. Particles size increase assisted enhancement of thermoluminescence emission in gadolinium and dysprosium oxide doped phosphate glasses. *Journal of Alloys and Compounds.* 2020;839:155479. https://doi.org/10.1016/j.jallcom.2020.155479

[12] Gavhane KH, Bhadane MS, Kulkarni PP, Bhoraskar VN, Dhole SD, Dahiwale SS. Investigation of novel Eu doped $SrDy_2O_4$ microphosphor for thermoluminescence dosimetry. *Journal of Luminescence.* 2021;231:117781. https://doi.org/10.1016/j.jlumin.2020.117781

[13] Sarikci S, Topaksu M, Madkhali O, Can N. Thermoluminescence characteristics and kinetic analyses of europium doped strontium gadolinium oxide phosphor. *Applied Radiation Isotopes.* 2023;191:110549. https://doi.org/10.1016/j.apradiso.2022.110549

[14] Saharin NS, Ahmad NE, Tajuddin HA, Tamuri AR. Thermoluminescence properties of aluminium oxide doped strontium, lithium and germanium prepared by combustion synthesis method. *EPJ Web Conference* 2017;156:00001. https://doi.org/10.1051/epjconf/201715600001

[15] Salleh NA, Tamuri AR, Saeed MA. Effect of strontium concentration on thermoluminescence glow curve of copper doped lithium magnesium borate glass. *Malaysian Journal of Fundamental Applied Sciences* 2017;13(3):275–8. https://doi.org/10.11113/mjfas.v13n3.570

[16] Rezaee Ebrahim Saraee K, Lotfi M. Gamma ray dosimetric properties of Tb- and Dy-doped $Ba_{0.88}Sr_{0.12}SO_4$ phosphor. *Iranian Journal of Science and Technology Transactions A: Science.* 2020;44:1549–58. https://doi.org/10.1007/s40995-020-00945-w

[17] Mohamed S, Salama E, Alazab HA, Bakry A, Sharma A, Assran Y. Synthesis and characterization of high-sensitivity Dy,Eu co-doped $CaSO_4$ thermoluminescent phosphor using coprecipitation technique. *Luminescence*. 2024;39(1):e4679. https://doi.org/10.1002/bio.4679

[18] Guckan V, Bereket S, Altunal V, Abusaid W, Yegingil Z. Luminescence properties of Tb and Eu activated $CaSO_4$ phosphor. *Radiation Physics and Chemistry.* 2023;203:110620. https://doi.org/10.1016/j.radphyschem.2022.110620

[19] Silva AMB, Rodrigues DS, Guedes BDO, Silveira IS, Antonio PL, Junot DO, et al. Exploring the luminescence properties and dosimetric characteristics of $CaSO_4$:Tb, $CaSO_4$:Mn, and $CaSO_4$:Mn,Tb phosphors synthesized by slow evaporation route. *Radiation Measurements.* 2024;177:107261. https://doi.org/10.1016/j.radmeas.2024.107261

[20] Silva AMB, Junot DO, Antonio PL, Souza DN, Caldas LVE. Analysis of dosimetric characteristics of $CaSO_4$:Mn,Tb phosphors synthesized by four different routes. *Applied Radiation Isotopes.* 2026;229:112381. https://doi.org/10.1016/j.apradiso.2025.112381

[21] Almasifard F, Zahedifar M. Thermoluminescence dosimetry characteristics of $MgSO_4$:Eu microcrystalline in gamma radiation. *Radiation Physics and Chemistry.* 2025;232: 112606. https://doi.org/10.1016/j.radphyschem.2025.112606

[22] Naeem HS, Mustafa IS, Yusof NN, Thabit HA, Mhareb MHA, Alajerami YSM, et al. High sensitivity transparent glass ceramic systems development based on $MgSO_4$:$Dy_2O_3$–$B_2O_3$ and $MgSO_4$:$Dy_2O_3$–$B_2O_3$:ZnO: an investigation of FT-IR and thermal properties for thermoluminescence dosimeter applications. *Optical Materials.* 2024;156:116003. https://doi.org/10.1016/j.optmat.2024.116003

[23] Naeem HS, Mustafa IS, Yusof NN, Raypah ME, Thabit HA, Mhareb MHA, et al. Altering the optical, physical, and TL dosimetric properties of $MgSO_4$:$Dy_2O_3$:$B_2O_3$ transparent glass ceramic system: evaluating the impact of roughness control and ZnO inclusion. *Journal of Non-Crystalline Solids. X*. 2024;22:100212. https://doi.org/10.1016/j.nocx.2024.100212

[24] Shannon RD. Revised effective ionic radii and systematic studies of interatomic distances in halides and chalcogenides. *Acta Crystallographica A*. 1976;32(5):751–67. https://doi.org/10.1107/S0567739476001551

[25] Saraswathi AV, Naregundi K, Sayyed MI, Almousa N, Kamath SD. Influence of annealing temperature on the structural and luminescence features and thermoluminescence trap parameters of $Ca_2Al_2SiO_7$:$Ce^{3+}$ phosphors. *JOM*. 2024;76(1):566–77. https://doi.org/10.1007/s11837-023-06184-9

[26] Girão AV, Caputo G, Ferro MC. Application of scanning electron microscopy–energy dispersive X-ray spectroscopy (SEM-EDS). *Comprehensive Analytical Chemistry.* 2017;75:153–68. https://doi.org/10.1016/bs.coac.2016.10.002

[27] Bakhsh M, Yasuda H, Ahmad N, Wong JHD, Mustafa IS. Zinc-doped magnesium borate glass: a potential thermoluminescence dosimeter for extended range of dosimetric applications. *Applied Sciences.* 2022;12(15):7491. https://doi.org/10.3390/app12157491

[28] Terada K, Nakamura S, Nakao T, Kimura A, Iwamoto O, Harada H, et al. Measurements of gamma-ray emission probabilities of $^{241,243}$Am and $^{239}$Np. *Journal of Nuclear Science and Technology.* 2016;53(11):1881–8. https://doi.org/10.1080/00223131.2016.1174167